Contract No:

This document was prepared in conjunction with work accomplished under Contract No. DE-AC09-08SR22470 with the U.S. Department of Energy (DOE) Office of Environmental Management (EM).

Disclaimer:

We put science to work.™

Savannah River National Laboratory®

OPERATED BY SAVANNAH RIVER NUCLEAR SOLUTIONS

A U.S. DEPARTMENT OF ENERGY NATIONAL LABORATORY • SAVANNAH RIVER SITE • AIKEN, SC

Geochemical Model of E_h and pH Transitions in Pore Fluids during Saltstone and SDU Concrete Aging

Saltstone Disposal Facility PA Revision

J. A. Dyer

October 2018

SRNL-STI-2018-00586

SRNL.DOE.GOV

DISCLAIMER

Printed in the United States of America

Prepared for
U.S. Department of Energy

SRNL-STI-2018-00586
Revision 0

Keywords: *Z-Area, Performance Assessment*

Retention: *Permanent*

Geochemical Model of E_h and pH Transitions in Pore Fluids during Saltstone and SDU Concrete Aging

Saltstone Disposal Facility PA Revision

J. A. Dyer

October 2018

Prepared for the U.S. Department of Energy under contract number DE-AC09-08SR22470.

Savannah River National Laboratory™
OPERATED BY SAVANNAH RIVER NUCLEAR SOLUTIONS

REVIEWS AND APPROVALS

AUTHORS:

_____

J. A. Dyer, Environmental Modeling, SRNL Date

TECHNICAL REVIEW:

_____

J. O. Dickson, Geosciences, SRNL Date

APPROVAL:

_____

D. A. Crowley, Manager Date
Environmental Modeling, SRNL

_____

L. T. Reid, Director Date
Environmental Restoration Technology, SRNL

_____

K. H. Rosenberger, Manager Date
Closure and Disposal Assessment

EXECUTIVE SUMMARY

The chemical and physical properties of the cementitious materials (dry cement, blast furnace slag, and fly ash) used to construct the Saltstone Disposal Units (SDUs) and saltstone waste form play a key role in the design and long-term performance of the Saltstone Disposal Facility. Chemical degradation of the reducing saltstone and concrete over time will impact radionuclide release and transport due to the changing chemical composition of groundwater (GW) percolating through the porous saltstone waste form. An equilibrium reaction path model was developed using The Geochemist's Workbench® (GWB) software to estimate the timescales (expressed as number of pore volumes) for chemical degradation of the reducing cementitious materials as indicated by changes in redox potential (E_h) and pH.

Bulk and mineral densities, porosity, and reducing capacities for saltstone and SDU concrete were based on an analysis of historical data generated by SIMCO Technologies Inc., Savannah River Ecology Laboratory, and Savannah River National Laboratory since 2008. The solid-phase mineralogies assumed for saltstone and SDU 2/6/7 concrete in the GWB simulations were determined via a normative analysis of the dry mix recipes and corresponding elemental analyses of the dry ingredients using Microsoft® Excel. Three different GW infiltration scenarios were considered for the saltstone waste form simulations: GW at pH 5.4, GW at pH 8.04 (aged concrete), and GW at pH 11.04 (unaged concrete). For SDU 2/6/7 concrete, only GW at pH 5.4 was considered. All simulations were performed using the **React** application within the GWB Professional 10.0.10 software.

GWB **React** model simulations were conducted for nine saltstone cases (GW at pH 5.4, 8.04, and 11.04, each with a saltstone reducing capacity of 350, 500, and 650 µeq/g), and three SDU 2/6/7 concrete cases (GW at pH 5.4 with a saltstone reducing capacity of 178, 209, and 239 µeq/g). The **React** simulations considered advective flow only and were executed in "flush" mode (i.e., an entering reactant fluid displaces an equal volume of previously equilibrated fluid from the system).

Table 0-1 presents a condensed summary of E_h and pH transitions predicted by the GWB reaction path model for saltstone and SDU 2/6/7 concrete. Interestingly, GWB predicts little difference in saltstone's E_h and pH transition profiles for the three GW scenarios. In addition, pH transition profiles for both saltstone and SDU 2/6/7 concrete are essentially insensitive to the assumed solid-phase reducing capacity. The E_h and Region III-to-IV pH transitions for saltstone occur approximately four to six times earlier than they do for SDU 2/6/7 concrete, mainly because of saltstone's six times greater porosity which is partially offset by the 5% to 45% greater mass of pyrrhotite and calcium silicate hydrate (CSH) for saltstone compared to SDU concrete.

Key uncertainties in the GWB model include assumptions associated with chemical equilibrium vs. rate-limited transformations, congruent vs. incongruent dissolution of CSH, homogeneous vs. heterogeneous distribution of blast furnace slag in saltstone, complete vs. partial hydration of cementitious minerals, and degradation of cementitious materials via other chemical processes including sulfate attack, carbonation-influenced steel corrosion, and decalcification. These uncertainties will likely have a moderate impact on the predicted E_h and pH transitions.

Table 0-1. Predicted E_h and pH Transitions for Saltstone and SDU 2/6/7 Concrete.

Case	E_h Transition				pH Transition	
	Value Range (mV)	Defensible Estimate (Pore Vol.)	Compliance Estimate (Pore Vol.)	Best Estimate (Pore Vol.)	Value Range (mV)	Pore Volume
Saltstone (all GW scenarios)	-660 to +566	600	850	1100	11.8 to 11.0 (Region I to III)	6
					11.8 to 9.1 (Region III to IV)	1400
SDU 2/6/7 Concrete (GW pH 5.4)	-660 to +565	3400	4000	4600	11.1 to 10.5 (Region III)	5850
					11.1 to 9.1 (Region III to IV)	7600

TABLE OF CONTENTS

LIST OF TABLES viii
LIST OF FIGURES ix
LIST OF ABBREVIATIONS x
1.0 Introduction 1
2.0 GWB Simulation Model Approach 1
2.1 Reducing Capacity Assumptions 3
2.2 Density and Porosity Assumptions 4
2.3 Mineralogy Assumptions 4
2.4 Infiltrating Groundwater 9
2.5 GWB **React** Simulation Cases 10
2.6 Quality Assurance 11
3.0 Results and Discussion 12
3.1 Saltstone Observations 12
3.2 SDU 2/6/7 Concrete Observations 16
3.3 Model Limitations 18
4.0 Conclusions 18
5.0 References 20

LIST OF TABLES

Table 0-1. Predicted E_h and pH Transitions for Saltstone and SDU 2/6/7 Concrete. vi

Table 2-1. Reducing Capacity of Saltstone and SDU 2/6/7 Concrete assumed in GWB React Model Simulations. 4

Table 2-2. Densities and Porosity of Saltstone and SDU 2/6/7 Concrete used in GWB React Model Simulations. 4

Table 2-3. Dry Mix Recipes used in Normative Analysis to Calculate Mineralogy for GWB Simulations. 6

Table 2-4. Normalized Average Chemical Composition of Individual Dry Ingredients based on SIMCO and SRNL Elemental Analyses. 6

Table 2-5. Normalized Average Chemical Composition of Dry Mixes for Saltstone and SDU 2/6/7 Concrete. 7

Table 2-6. Heuristics used to Generate Mineralogical Compositions for GWB Simulations. 7

Table 2-7. Normalized Mineralogical Compositions used in GWB React Model Simulations. 8

Table 2-8. Supplementary Thermodynamic Data for Cement Phases. 8

Table 2-9. GWB-Predicted Groundwater Infiltrate Stream Compositions for Saltstone and SDU 2/6/7 Concrete Simulations on a Concentration (mg/L) Basis. 10

Table 2-10. GWB-Predicted Groundwater Infiltrate Stream Compositions for Saltstone and SDU 2/6/7 Concrete Simulations on a Moles-of-Constituent Basis. 11

Table 3-1. GWB-Predicted Redox Potential (E_h) Transitions for Saltstone and SDU 2/6/7 Concrete. 13

Table 3-2. GWB-Predicted pH Transitions for Saltstone and SDU 2/6/7 Concrete. 14

Table 4-1. Predicted E_h and pH Transitions for Saltstone and SDU 2/6/7 Concrete. 19

LIST OF FIGURES

Figure 2-1. GWB Professional 10.0.10 React Model Input GUIs. 2

Figure 2-2. Selection of Flush Mode in Config → Stepping Dialog Box..... 3

Figure 2-3. Schematic Representation of Flush Mode in GWB Professional 10.0.10 React Application.... 3

Figure 3-1. Redox Potential vs. Number of Pore Volumes of pH 5.4 Groundwater Reacted with Saltstone. 15

Figure 3-2. pH vs. Number of Pore Volumes of Different Groundwaters Reacted with Saltstone. 15

Figure 3-3. pH vs. First Ten Pore Volumes of pH 5.4 Groundwater Reacted with Saltstone. 16

Figure 3-4. Redox Potential vs. Number of Pore Volumes of pH 5.4 Groundwater Reacted with SDU 2/6/7 Concrete..... 17

Figure 3-5. pH vs. Number of Pore Volumes of pH 5.4 Groundwater Reacted with SDU 2/6/7 Concrete. 17

LIST OF ABBREVIATIONS

atm	atmosphere
BFS	blast furnace slag
CSH	calcium silicate hydrate
cu. yd.	cubic yard
E_h	redox potential
η	porosity
g	gram mass
GW	groundwater
GUI	graphical user interface
GWB	The Geochemist's Workbench®
lb	pound by weight
kg	kilogram mass
LOI	Loss on Ignition
m^3	cubic meter
mg/L	milligram per liter
µeq	microequivalent
PA	Performance Assessment
ρ_b	bulk density
ρ_m	mineral density
SDF	Saltstone Disposal Facility
SDU	Saltstone Disposal Unit
SIMCO	SIMCO Technologies Inc.
SREL	Savannah River Ecology Laboratory
SRNL	Savannah River National Laboratory
SRR	Savannah River Remediation
SRS	Savannah River Site
XRD	X-ray diffraction

1.0 Introduction

The Saltstone facilities stabilize and dispose of low-level radioactive salt solution originating from the liquid-waste storage tanks at the Department of Energy's Savannah River Site (SRS). The Saltstone Production Facility, located in Z-Area at SRS, receives treated aqueous salt solution and mixes the waste with dry cement, blast furnace slag (BFS), and fly ash to form a grout slurry that is mechanically pumped into concrete disposal cells that compose the Saltstone Disposal Facility (SDF). The solidified grout formed in this process is called "saltstone" (Flach, 2018).

The chemical and physical properties of the cementitious materials (dry cement, BFS, and fly ash) play a key role in the design and long-term performance of the SDF. The saltstone grout serves as a physical barrier to contaminant release because of its low permeability and diffusivity. The waste form also acts as a chemical barrier to contaminant release for radionuclides such as Tc-99, whose solubility and mobility are a function of the reducing capacity of the grout (Flach, 2018).

Similarly, the concrete shell of the saltstone disposal unit (SDU) serves as an added physical and chemical barrier to radionuclide release (Flach, 2018). Considered together, the saltstone waste form and the SDU represent a robust containment structure at facility closure. However, the physical and chemical properties of the cementitious materials will change over time via sulfate attack, carbonation-influenced steel corrosion, and decalcification. During the thousands of years of interest in a Performance Assessment (PA), barrier performance will degrade (Flach, 2018).

Degradation of the reducing saltstone and concrete used to construct the SDUs will dictate the evolving chemical composition of the aqueous pore fluid percolating through the porous saltstone waste form, affecting contaminant release. Geochemical equilibrium model simulations were performed using The Geochemist's Workbench® (GWB) software (Aqueous Solutions LLC, 2016) to estimate the timescales for chemical degradation of the reducing cementitious materials as indicated by changes in redox potential (E_h) and pH. The timescales for the E_h and pH transitions are expressed as pore volumes of reacting fluid passing through the saltstone waste form or concrete.

The GWB simulations do not directly consider physical degradation (e.g., fracturing), although physical degradation will likely affect the rate of chemical degradation by influencing the rate at which porewater passes through the cementitious materials. In addition, the GWB model assumes chemical equilibrium, meaning that all dissolution, precipitation, and redox transformation reactions go to completion. This is a reasonable assumption given the expected timeframe for degradation (many hundreds to many thousands of years) and the very low infiltration rates expected for the final cover system.

2.0 GWB Simulation Model Approach

The release and subsequent transport of radionuclides from the SDUs depend on two master variables: pH and reduction potential (E_h). As the saltstone and concrete age, the pH and E_h of the pore fluids in equilibrium with minerals comprising the saltstone and SDU concrete solids will

change over time. Because equilibrium is assumed, the pH and E_h transitions predicted by the GWB model will occur as sharp step changes, rather than gradual changes over a more extended time.

All simulations were performed using the **React** application within The Geochemist's Workbench® Professional 10.0.10 software (Aqueous Solutions LLC, 2016). **React** is a reaction path model for simulating vapor-liquid-solid equilibrium states and geochemical processes (precipitation, dissolution, complexation, volatilization) in aqueous systems. Figure 2-1 displays screen captures of the GWB Professional 10.0.10 Apps homepage where the **React** application is launched as well as the three main **React** input-parameter graphical user interfaces (GUIs).

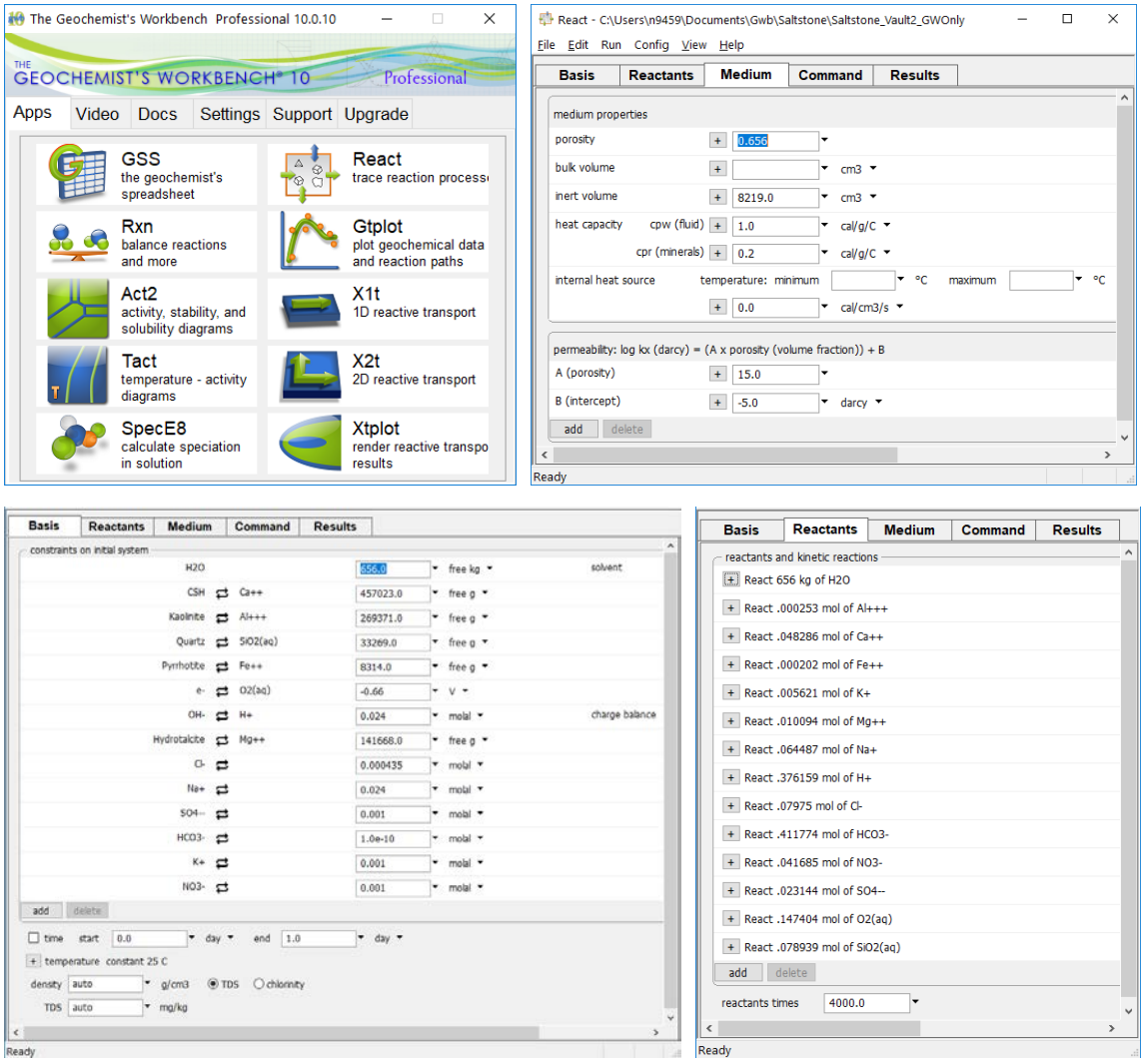

Figure 2-1. GWB Professional 10.0.10 React Model Input GUIs.

React simulations were executed in "flush" mode (Figure 2-2) where an entering reactant fluid displaces an equal volume of existing equilibrated fluid from the system. A flush model is traced from the frame of reference of the porous "rock" matrix through which the aqueous fluid migrates.

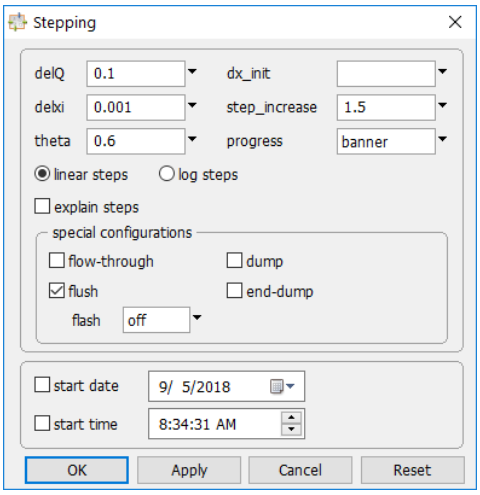

Figure 2-2. Selection of Flush Mode in Config → Stepping Dialog Box.

As shown in Figure 2-3, each pore volume (*n*) of Z-Area groundwater infiltrate is equilibrated with the cementitious minerals in saltstone or SDU concrete, displacing one pore volume (*n* - 1) of existing previously equilibrated porewater. All transport of dissolved ions is assumed to occur because of the advective flow of infiltrating groundwater. In addition, because the initial saltstone and SDU concrete pore fluids are flushed from the system with the first pore volume of groundwater infiltrate, limitations in the accuracy of the extended Debye-Hückel aqueous-activity-coefficient model used by GWB at high ionic strength are avoided (Denham, 2008).

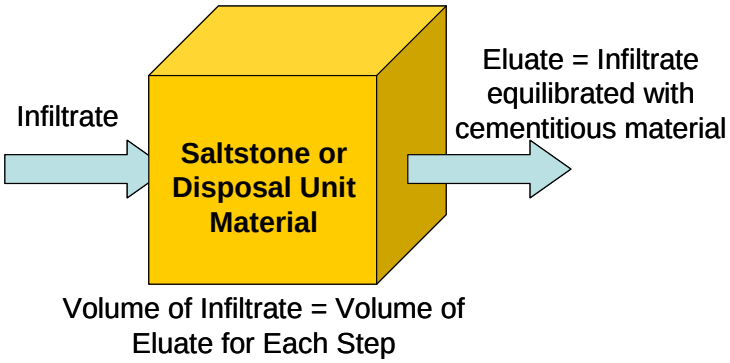

Figure 2-3. Schematic Representation of Flush Mode in GWB Professional 10.0.10 React Application (after Denham, 2008).

The approach described below was taken to generate the GWB input parameters, perform the GWB **React** model simulations, and process the model output.

2.1 Reducing Capacity Assumptions

After an analysis of historical experimental data from SRNL and Savannah River Ecology Laboratory (SREL), Hommel and Dixon (2018) proposed and reached consensus with others in SRNL on the assumed reducing capacity of saltstone for the Defensible (defense-in-depth), Compliance (most probable and defensible), and Best-Estimate (realistic) uncertainty cases. The assumed reducing capacity of SDU 2/6/7 concrete for the Defensible, Compliance, and Best-

Estimate uncertainty cases are based on data previously reported by Roberts and Kaplan (2009) in Table 2 of their report. Table 2-1 lists the reducing capacity of saltstone and SDU 2/6/7 concrete assumed in the GWB model simulations. The reducing capacities, as measured, were based on the total mass of the saltstone and concrete samples (i.e., sodium salts from the salt waste are included in the sample mass used to calculate the reducing capacity in µeq/g sample).

Table 2-1. Reducing Capacity of Saltstone and SDU 2/6/7 Concrete assumed in GWB React Model Simulations.

Solid Type	Defensible Case (µeq/g)	Compliance Case (µeq/g)	Best-Estimate Case (µeq/g)
Saltstone	350	500	650
SDU 2/6/7 Concrete	178	209	239

The mineral in BFS that is responsible for its reducing capacity is assumed to be pyrrhotite (FeS). Pyrrhotite is a highly reduced, high-temperature mineral phase potentially generated during the formation of BFS and has been identified in various smelting slags (Zainoun et al., 2003; Muszer, 2006; Gupta et al., 2007). The relevant oxidation-reduction reaction for pyrrhotite is:

$$FeS_{(s)} + 2O_{2(aq)} = Fe^{2+} + SO_4^{2-}$$

Eight (8) electron equivalents are transferred for every mole of pyrrhotite oxidized, which equates to 91,000 microequivalents per gram (µeq/g) of FeS. This conversion factor, together with the reducing capacities assumed in Table 2-1, enables calculation of the mass concentration of pyrrhotite for each case as described in Section 0 below.

2.2 Density and Porosity Assumptions

Bulk density (ρ_b), mineral density (ρ_m), and porosity (η) for saltstone and SDU 2/6/7 concrete were based on an analysis of historical data from both SIMCO Technologies Inc. (SIMCO) and SREL as reported by Hommel (2018). Table 2-2 summarizes the recommended parameter values used in the GWB model simulations. The bulk density of saltstone does not include the sodium salts from the salt waste which amount to approximately 232 kg/m^3.

Table 2-2. Densities and Porosity of Saltstone and SDU 2/6/7 Concrete used in GWB React Model Simulations.

Solid Type	Mineral Density (ρ_m) (kg/m^3)	Bulk Density (ρ_b) (kg/m^3)	Porosity (η) (m^3 pores/m^3 total)
Saltstone	2720	932 *	0.656
SDU 2/6/7 Concrete	2449	2180	0.11

* The bulk density of saltstone would equal 1164 kg/m^3 if sodium salts from salt waste are included.

2.3 Mineralogy Assumptions

A method was required for deriving the mineralogy of saltstone and SDU concrete that is compatible with the GWB thermodynamic framework because quantitative measurements of the exact mineralogy are not available. To be consistent with the 2009 Saltstone PA, a normative analysis method like the one described by Denham (2008) was employed in this work. The mineralogy was based on elemental chemical analyses of components that comprise the

cementitious forms and checked for consistency with X-ray powder diffraction data generated by Langton and Missimer (2014) for different hydrated blends of cement, slag, fly ash, and salt.

As described below, a normative analysis was performed for both saltstone and SDU 2/6/7 concrete using the dry mix recipes and corresponding elemental analyses of the dry ingredients to determine an assumed solid-phase mineralogy for the GWB simulations.

- Dry mix recipes for saltstone and SDU 2/6/7 concrete selected for the GWB simulations are summarized in Table 2-3 following a review of dry mix recipes included in seven historical SIMCO and SRR documents.
- Normalized average chemical compositions based on SRNL and SIMCO elemental analyses from 2006 through 2012 were calculated for the dry-mix binders (cement, BFS, fly ash, and silica fume) and are reported in Table 2-4. Appendix A provides tables summarizing elemental analyses of the individual samples used to arrive at the normalized average values for the four dry binders.
- Using the dry mix recipes in Table 2-3 and the normalized average chemical composition for each dry ingredient in Table 2-4, an overall normalized average chemical composition was calculated for both saltstone and SDU 2/6/7 concrete as shown in Table 2-5.
- Table 2-6 presents a set of heuristics originally adopted by Denham (2008) to transform the dry-mix chemical compositions for saltstone and SDU 2/6/7 concrete into an assumed hydrated mineralogy for the GWB simulations. Hydration of the dry mix is assumed to be 100 percent; incomplete hydration would lower the neutralization and reducing capacities of the saltstone and SDU concrete.
- The assumed hydrated mineralogy was compared to X-ray diffraction (XRD) data reported by Langton and Missimer (2014) to ensure consistency. Most importantly, Tables 8 through 10 in their report confirm: (1) the absence of $Ca(OH)_2$ (portlandite) in all cementitious material blends that include slag and/or fly ash, and (2) the presence of CSH, hydrotalcite, quartz, and possibly Ca-carboaluminate in the saltstone waste form (cement + slag + fly ash + salt solution). One difference between the normative analysis and XRD data is the identity of the aluminosilicate mineral. XRD spectra identified the presence of mullite ($Al_6Si_2O_{13}$), which forms at temperatures above 1200 ^oC and originates with the fly ash, while the normative analysis assumes the presence of kaolinite ($Al_2Si_2O_5(OH)_4$). Because neither mineral impacts the reducing and neutralization capacities of saltstone and SDU concrete to any appreciable extent, kaolinite was retained in the normative analysis and GWB model.
- Lastly, the hydrated mineralogical compositions for saltstone and SDU concrete were normalized to the assumed reduction capacities and bulk densities listed in Table 2-1 and Table 2-2, respectively. For each iteration, all mineral concentrations (including pyrrhotite) were first normalized to the assumed bulk density (932 kg/m^3 for saltstone and 2180 kg/m^3 for SDU 2/6/7 concrete). The pyrrhotite (FeS) concentration was then normalized a second time to the assumed reducing capacities using a bulk density of 1164 kg/m^3 for saltstone and 2180 kg/m^3 for SDU 2/6/7 concrete. As noted in Section 2.1, the reducing capacities, as measured, include the mass of the sodium salts from the salt waste.

Three iterations were adequate to arrive at the final normalized hydrated mineralogical compositions used in the GWB simulations, which are summarized in Table 2-7.

Table 2-3. Dry Mix Recipes used in Normative Analysis to Calculate Mineralogy for GWB Simulations.

Ingredient	Saltstone [a] (lb./cu. yd. final product)	Saltstone Dry Binders Fraction	SDU 2/6/7 Concrete [b] (lb./cu. yd. final product)	SDU 2/6/7 Dry Binders Fraction
Type II Cement	158	0.10		
Type V Cement			213	0.30
Holcim BFS	713	0.45		
Lehigh BFS			284	0.40
Type F Fly Ash	713	0.45	163	0.23
Silica Fume			50	0.07
Inerts				
Sand			1048	
Aggregate			1795	
$NaNO_3$ Salt	391			
Dry Mix Total (lb/cu. yd.)	1975		3553	
Dry Mix Total (kg/m^3)	1172		2108	
Water-to-Cement Mass Ratio (kg/kg)	0.60		0.38	
Water	951		269.5	

[a] SIMCO Technologies Inc. (2010)

[b] C-SPP-Z-00015 (2017)

Table 2-4. Normalized Average Chemical Composition of Individual Dry Ingredients based on SIMCO and SRNL Elemental Analyses.

Oxide	Cement (g/100 g cement)	Blast Furnace Slag (g/100 g BFS)	Fly Ash (g/100 g fly ash)	Silica Fume (g/100 g silica)
CaO	64.79	36.84	1.02	0.60
SiO_2	20.94	39.32	55.34	94.78
Al_2O_3	4.87	8.19	28.78	0.18
Fe_2O_3	3.87	0.38	7.15	0.07
SO_3	2.43	1.64	0.10	0.18
MgO	1.41	12.72	0.98	0.22
K_2O	0.55	0.39	2.76	0.48
Na_2O	0.15	0.28	0.39	0.18
TiO_2	0.30	0.35	1.52	0.00
LOI* / Volatiles	0.66	-0.11	1.95	3.31
Total	100.00	100.00	100.00	100.00

* Loss on Ignition

Table 2-5. Normalized Average Chemical Composition of Dry Mixes for Saltstone and SDU 2/6/7 Concrete.

Oxide	Molecular Weight (g/mole)	Saltstone (g/kg dry mix)	Saltstone (mole/kg dry mix)	SDU 2/6/7 Concrete (g/kg dry mix)	SDU 2/6/7 Concrete (mole/kg dry mix)
CaO	56.08	188.52	3.37	68.84	1.23
SiO_2	60.08	358.49	5.98	82.71	1.38
Al_2O_3	101.96	137.39	1.35	22.70	0.22
Fe_2O_3	159.69	30.29	0.19	5.92	0.037
SO_3	80.07	8.22	0.10	2.84	0.035
MgO	40.30	50.62	1.27	11.50	0.29
Inert A [a]	N/A	28.49	N/A	5.32	N/A
Inert B [b]	N/A	198.0	N/A	0.00	N/A
Inert C [c]	N/A	0.00	N/A	800.2	N/A
Total	N/A	1000.0	N/A	1000.0	N/A

[a] Inert A includes the soluble salts K_2O, Na_2O, and TiO_2 plus LOI/volatiles.

[b] Inert B includes sodium nitrate salts originally precipitated in the saltstone waste form that are assumed to solubilize and quickly flush out of the porous saltstone matrix.

[c] Inert C consists of aggregate and sand in the SDU concrete.

Table 2-6. Heuristics used to Generate Mineralogical Compositions for GWB Simulations.

Oxide	Assumed Mineral(s)	Heuristic
CaO	Primary: $CaSiO_3 \cdot H_2O$ (calcium silicate hydrate or CSH)	All calcium and stoichiometric silicon to CSH.
SiO_2	Primary: $CaSiO_3 \cdot H_2O$ (calcium silicate hydrate or CSH) Balance: SiO_2 (quartz)	Stoichiometric silicon to CSH; balance to quartz.
Al_2O_3	Primary: $Mg_4Al_2O_7 \cdot 10(H_2O)$ (hydrotalcite) Balance: $Al_2Si_2O_5(OH)_4$ (kaolinite) or $Al(OH)_3$ (gibbsite)	Stoichiometric aluminum to hydrotalcite; balance to kaolinite (saltstone) and gibbsite (SDU 2/6/7 concrete).
Fe_2O_3	Primary: FeS (pyrrhotite) Balance: Fe_2O_3 (inert hematite)	Stoichiometric iron to pyrrhotite; balance to hematite (considered as another inert in GWB simulations)
SO_3	Primary: FeS (pyrrhotite)	All sulfur and stoichiometric iron to pyrrhotite.
MgO	Primary: $Mg_4Al_2O_7 \cdot 10(H_2O)$ (hydrotalcite)	All magnesium and stoichiometric aluminum to hydrotalcite.

Table 2-7. Normalized Mineralogical Compositions used in GWB React Model Simulations.

Hydrated Mineral	Saltstone Cases			SDU 2/6/7 Concrete Cases		
	Defensible 350 µeq/g (g/m^3)	Compliance 500 µeq/g (g/m^3)	Best-Estimate 650 µeq/g (g/m^3)	Defensible 178 µeq/g (g/m^3)	Compliance 209 µeq/g (g/m^3)	Best-Estimate 239 µeq/g (g/m^3)
$CaSiO_3 \cdot H_2O$ (CSH)	458921	457972	457023	347233	347114	346999
$Mg_4Al_2O_7 \cdot 10(H_2O)$ (Hydrotalcite)	142256	141962	141668	66965	66942	66920
$Al_2Si_2O_5(OH)_4$ (Kaolinite)	270490	269930	269371	0	0	0
$Al(OH)_3$ (Gibbsite)	0	0	0	49546	49529	49512
SiO_2 (Quartz)	33407	33338	33269	18869	18862	18856
FeS (Pyrrhotite)	4477	6395	8314	4264	5007	5725
Total GWB Inerts[a]	22356	22403	22449	1693124	1692546	1691987
Total GWB Solids[b]	932000	932000	932000	2180000	2180000	2180000

[a] Total GWB Inerts include residual Fe_2O_3 only (Table 2-6) for saltstone and Inert C (aggregate and sand) plus residual Fe_2O_3 (Table 2-6) for SDU concrete. Total GWB Inerts are unreactive solids whose mass is conserved in the **React** model simulations. Their inclusion in the model impacts the porosity of the rock matrix. Inert A (K_2O, Na_2O, TiO_2, and LOI/volatiles) in Table 2-4 and Inert B (sodium nitrate salts) in Table 2-5 are water soluble or volatile.

[b] Total GWB Solids should be equal to the bulk density reported in Table 2-2.

Thermodynamic data for five missing cement phases included in the model simulations were added to GWB's default thermodynamic database, *thermo.tdat*; the edited database file was renamed *thermo cement.tdat*. Table 2-8 displays the equilibrium dissolution reactions for the five added cement phases, together with the corresponding equilibrium constants and literature references. As used in this report, calcium silicate hydrate (CSH) refers to the compound with molecular formula $CaSiO_3 \cdot H_2O$. In the literature, C-S-H refers more broadly to a family of calcium silicate hydrate species with a variable molecular formula and, therefore, a differing dissolution reaction and Gibbs free energy of formation. For this study, the C-S-H dissolution model of Berner (1992) as presented by Park and Batchelor (2002) was employed. In the Berner model, C-S-H is a non-ideal mixture of two solid phases whose identity and respective solubility constant depend on the Ca/Si ratio. A Ca/Si ratio equal to 0.5, which lies at the lower end of possible C-S-H compositions, is assumed for saltstone and SDU concrete because of the low portlandite-to-fly-ash and portlandite-to-slag ratios used in the cementitious forms. Denham (2008) found that GWB simulations for the cases of interest in this report are not particularly sensitive to Ca/Si ratios less than or equal to 1.0.

Table 2-8. Supplementary Thermodynamic Data for Cement Phases.
(added to GWB default thermodynamic database *thermo.tdat*; database renamed *thermo cement.tdat*)

Cement Phase	Dissolution Reaction	Solubility Constant (log K)	Reference
CSH	$CaSiO_3 \cdot H_2O + 2H^+ = Ca^{+2} + SiO_{2(aq)} + 2H_2O$	15.15	Park and Batchelor (2002)
Hydrotalcite	$Mg_4Al_2O_7 \cdot 10H_2O + 14H^+ = 4Mg^{+2} + 2Al^{+3} + 17H_2O$	73.78	Bennett et al. (1992)
C4AH13	$Ca_4Al_2O_7 \cdot 13H_2O + 14H^+ = 4Ca^{+2} + 2Al^{+3} + 20H_2O$	100.77	Reardon (1990)
Ca-carboaluminate	$Ca_2Al_2O_4CO_3 \cdot 11H_2O + 9H^+ = 2Ca^{+2} + 2Al^{+3} + HCO_3^- + 15H_2O$	34.76	Reardon (1990)
Ettringite	$Ca_6Al_2O_6(SO_4)_3 \cdot 32H_2O + 12H^+ = 6Ca^{+2} + 2Al^{+3} + 3SO_4^{-2} + 38H_2O$	57.15	Reardon (1990)

2.4 Infiltrating Groundwater

The baseline groundwater (GW) composition used in the saltstone and SDU 2/6/7 concrete simulations is reported by Millings and Denham (2012) in Table 2, *Water Chemistries for P29D*, Case 4. Millings (2012) provides a summary of carbon dioxide (CO_2) partial pressures in water table wells and the vadose zone at SRS. In this study, baseline GW was assumed to be pH 5.4 in equilibrium with gaseous CO_2 at a partial pressure of 0.0137 atmospheres (atm). Total pressure and GW temperature were assumed to equal 1 atm and 20.8 ^oC, respectively.

Saltstone is encased in concrete so it was assumed that the origin of the infiltrate into the saltstone waste form was GW with and without interaction with the SDU concrete. As a result, three different GW infiltration scenarios were considered for the saltstone waste form simulations:

1. Baseline GW at pH 5.4 in equilibrium with CO_2 gas at a partial pressure of 0.01372 atm.
2. Equilibrated GW from Scenario No. 1 is re-equilibrated with excess calcite (oxidized concrete, aged). Under this scenario, the equilibrium pH increases to 8.04 and the partial pressure of CO_2 gas decreases to 0.00061 atm.
3. Equilibrated GW from Scenario No. 1 is re-equilibrated with excess CSH (oxidized concrete, unaged). Under this scenario, the equilibrium pH increases to 11.04 and the partial pressure of CO_2 gas decreases to 2.4E-10 atm.

The first scenario is relevant if preferential or “fast” flow through the SDU concrete allows unreacted GW to directly contact the saltstone matrix. The second scenario applies when GW equilibrates with aged, oxidized SDU concrete before contacting the saltstone matrix (Region III per Bradbury and Sarott, 1995; Region IV per Ochs et al., 2016). Finally, in the third scenario, infiltrating GW equilibrates with unaged, oxidized SDU concrete before contacting the saltstone matrix (Region II per Bradbury and Sarott, 1995; Region III per Ochs et al., 2016). For SDU 2/6/7 concrete, only Scenario No. 1 (Baseline GW) applies.

The **React** application in GWB 10.0.10 was used to generate charge-balanced GW infiltrate streams on a concentration (mg/L) basis for the three GW scenarios above as shown in Table 2-9. The infiltrate stream compositions were next transformed to a molar basis (total moles of each

Table 2-9. GWB-Predicted Groundwater Infiltrate Stream Compositions for Saltstone and SDU 2/6/7 Concrete Simulations on a Concentration (mg/L) Basis.

GWB Basis Species *	GW Scenario 1 Baseline GW pH 5.4 $p_{CO2(g)}$ = 0.01372 atm	GW Scenario 2 GW + Calcite pH 8.04	GW Scenario 3 GW + CSH pH 11.04
	GWB P29D Charge-Balanced Composition Millings & Denham (2012), Case 4	GWB Charge-Balanced Composition	GWB Charge-Balanced Composition
	mg/L	mg/L	mg/L
Al^{3+}	0.0104	0.0104	0.0104
Ca^{2+}	2.95	25.43	120.25
Fe^{2+}	0.0172	0.0172	0.0172
K^{+}	0.335	0.335	0.335
Mg^{2+}	0.374	0.374	0.374
Na^{+}	2.26	2.26	2.26
H^{+}	0.578	0.011	-5.944
Cl^{-}	4.31	4.31	4.43
HCO_3^{-}	38.3	72.4	0.43
NO_3^{-}	3.94	3.94	3.94
SO_4^{2-}	2.26	2.26	2.26
O_2 (aq)	7.19	7.19	7.19
SiO_2 (aq)	7.23	7.23	205.23

* The constituents listed in Column 1 are the "basis species" used in the GWB model input file. They do not represent the actual speciation in the infiltrate streams.

constituent) assuming a total (solid plus liquid) cell volume of one cubic meter and a porosity as reported in Table 2-2 of 0.656 m^3 pores/m^3 total for saltstone and 0.11 m^3 pores/m^3 total for SDU 2/6/7 concrete. Table 2-10 provides the GW infiltrate stream compositions on a moles-of-constituent basis as used in the GWB **React** model simulations.

2.5 GWB **React** Simulation Cases

GWB **React** simulations were executed for 12 cases:

- Nine saltstone cases (GW only, GW plus calcite, and GW plus CSH each at a reducing capacity of 350, 500, and 650 µeq/g).
- Three SDU 2/6/7 concrete cases (GW only at a reducing capacity of 178, 209, and 239 µeq/g).

The **React** simulations considered advective flow only (i.e., no diffusion), and as shown in Figure 2-3, were executed in "flush" mode where an entering reactant fluid displaces an equal volume of previously equilibrated fluid from the system. The **React** model output was exported to Microsoft Excel where post-processing converted the number of GWB reaction steps to the number of pore volumes of reacting fluid passing through the saltstone waste form or concrete.

Table 2-10. GWB-Predicted Groundwater Infiltrate Stream Compositions for Saltstone and SDU 2/6/7 Concrete Simulations on a Moles-of-Constituent Basis.

GWB Basis Species *	Saltstone Cases (η = 0.656)			SDU 2/6/7 Concrete Cases (η = 0.11)
	GW Scenario 1 Baseline GW pH 5.4 $p_{CO2(g)}$ = 0.01372 atm	GW Scenario 2 GW + Calcite pH 8.04	GW Scenario 3 GW + CSH pH 11.04	GW Scenario 1 Baseline GW pH 5.4 $p_{CO2(g)}$ = 0.01372 atm
	gram-moles	gram-moles	gram-moles	gram-moles
Al^{3+}	0.000253	0.000253	0.000253	0.000042
Ca^{2+}	0.048286	0.416238	1.968301	0.008097
Fe^{2+}	0.000202	0.000202	0.000202	0.000034
K^{+}	0.005621	0.005621	0.005620	0.000943
Mg^{2+}	0.010094	0.010094	0.010092	0.001693
Na^{+}	0.064487	0.064486	0.064474	0.010813
H^{+}	0.376159	0.007009	-3.868401	0.063075
Cl^{-}	0.079750	0.079742	0.081901	0.013373
HCO_3^{-}	0.411774	0.778623	0.004623	0.069047
NO_3^{-}	0.041685	0.041684	0.041677	0.006990
$SO4^{2-}$	0.023144	0.023143	0.023139	0.003881
O_2 (aq)	0.147404	0.147400	0.147375	0.024717
SiO_2 (aq)	0.078939	0.078937	2.240783	0.013237

* The constituents listed in Column 1 are the "basis species" used in the GWB model input file. They do not represent the actual speciation in the infiltrate streams.

The model was set up such that one reaction step is equivalent to one pore volume of advective flow. Between 4,000 and 10,000 pore volumes were needed to reach the desired transition points for E_h and pH.

2.6 Quality Assurance

The Software Quality Assurance Plan for Release 9.0.2 of The Geochemist's Workbench® software (Millings et al., 2012) was revisited and updated to cover Release 10.0.10 in accordance with minimum requirements for Level C purchased software owned by SRNL and as defined in the 1Q Quality Assurance Manual, Procedure 20-1, Rev. 19 and Manual E7, Procedure 5.01, Rev. 4 (Dyer, 2018).

A design check was also performed on the calculation and selection of the model input parameters, the implementation and execution of the **React** flush model in the GWB software for each of the four cases (three saltstone and one SDU 2/6/7 concrete), and the post-processing of the model output to arrive at the predicted number of pore volumes for each E_h and pH transition. A technical review of this report was also performed consistent with the E7 Manual, procedure

2.60 as outlined in SRNL Technical Report Design Checklist contained in WSRC-IM-2002-00011, Rev. 2.

3.0 Results and Discussion

Table 3-1 and Table 3-2 summarize the E_h and pH transition points of interest, respectively, for the 12 saltstone and SDU 2/6/7 concrete uncertainty cases. Included in the tables are the cumulative E_h and pH value ranges over which the respective transitions occur, the total (cumulative) number of pore volumes associated with the reported value ranges, and the dominant geochemical processes controlling the transition points. For E_h, the only transition of importance is the step change from -660 mV (reducing, sulfide-controlled) to +566/565 mV (oxidizing, O_2-controlled), which occurs when 100% of the reducing capacity (FeS) of saltstone and SDU 2/6/7 concrete is consumed by dissolved oxygen in the GW infiltrate.

On the other hand, two transitions (step changes) are reported for pH. For saltstone, the first transition represents the predicted change from cement degradation Region I to Region III as defined by Ochs et al. (2016) in the footnote for Table 3-2. This first transition (from pH 11.8 to pH 11) is potentially of significance because the anticipated long-term infiltration rate through the planned SDF closure cap is two orders of magnitude lower than assumed in the 2009 PA based on new findings by Benson and Benavides (2018). On the contrary, the first transition for SDU concrete (from pH 11.1 to pH 10.5) does not represent a switch in the cement degradation region but rather a change in geochemical control from CSH buffered to Ca-carboaluminate buffered. The second pH transition for both saltstone and SDU concrete is more significant because it represents a loss in the acid neutralization capacity of the solid matrix and a transition from cement degradation Region III to IV as defined by Ochs et al. (2016). The main reaction driving the transition from Region III (CSH buffered) to Region IV (calcite buffered) is the consumption of CSH by carbon dioxide acidity in the GW infiltrate stream to produce calcite via the net overall reaction: $CaSiO_3 \cdot H_2O_{(s)} + H_2CO_{3(aq)} = CaCO_{3(s)} + SiO_{2(aq)} + 2H_2O$.

3.1 Saltstone Observations

The modeling results show little differentiation in the E_h and pH transition points for the three different GW compositions/conditions. The E_h transitions do not vary because all three GW infiltrate streams are assumed to have the same dissolved oxygen concentration of 7.2 mg/L (i.e., streams are saturated with respect to oxygen in air at 1 atm total pressure and 20.8 ^oC). Figure 3-1 displays the E_h profiles for saltstone reacted with GW at pH 5.4 for the Defensible, Compliance, and Best-Estimate Reducing-Capacity scenarios. The graphs for saltstone reacted with GW + calcite (pH 8.04) and GW + CSH (pH 11.04) are essentially identical to Figure 3-1 (see Appendix B).

As shown in Figure 3-2, the pH profiles for saltstone are also identical for GW (pH 5.4) and GW + Calcite (pH 8.04) because total acidity (i.e., the sum of proton, carbon dioxide, aluminum, and ferric iron acidity) in both streams is essentially equal. On the other hand, a step change in pH does not occur for the GW + CSH (pH 11.04) scenario because the GW infiltrate is already saturated with respect to CSH from percolating through the SDU concrete, substantially limiting the dissolution rate of CSH in saltstone (see Figure 3-2).

Table 3-1. GWB-Predicted Redox Potential (E_h) Transitions for Saltstone and SDU 2/6/7 Concrete.

Saltstone Case	**Value Range (mV)**	**Defensible Estimate 350 µeq/g (Pore Volumes)**	**Compliance Estimate 500 µeq/g (Pore Volumes)**	**Best Estimate 650 µeq/g (Pore Volumes)**	**Geochemical Controls on Transition**
GW at pH 5.4 (no fluid contact with concrete)	-660 to +566	600	850	1100	Pyrrhotite consumed
GW + Calcite at pH 8.04 (oxidized concrete, aged; Region IV per Ochs et al., 2016)	-660 to +566	600	850	1100	Pyrrhotite consumed
GW + CSH at pH 11.04 (oxidized concrete, unaged; Region III per Ochs et al., 2016)	-660 to +566	615	865	1115	Pyrrhotite consumed
SDU 2/6/7 Concrete Case	**Value Range (mV)**	**Defensible Estimate 178 µeq/g (Pore Volumes)**	**Compliance Estimate 209 µeq/g (Pore Volumes)**	**Best Estimate 239 µeq/g (Pore Volumes)**	**Geochemical Controls on Transition**
GW at pH 5.4	-660 to +565	3415	4000	4570	Pyrrhotite consumed

Table 3-2. GWB-Predicted pH Transitions for Saltstone and SDU 2/6/7 Concrete.

Saltstone Case	**Value Range (pH)**	**Defensible Estimate 350 µeq/g (Pore Volumes)**	**Compliance Estimate 500 µeq/g (Pore Volumes)**	**Best Estimate 650 µeq/g (Pore Volumes)**	**Geochemical Controls on Transition [1]**
GW at pH 5.4 (no fluid contact with concrete)	11.8 to 11.0	6	6	6	Region I to III: CSH + Increasingly calcite buffered. Region II (portlandite) negligible because Ca/Si < 1.0.
	11.8 to 9.1	1410	1400	1390	Region III to IV: CSH consumed; calcite buffered.
GW + Calcite at pH 8.04 (oxidized concrete, aged; Region IV per Ochs et al., 2016)	11.8 to 11.0	6	6	6	Region I to III: CSH + Increasingly calcite buffered. Region II (portlandite) negligible because Ca/Si < 1.0.
	11.8 to 9.1	1410	1400	1390	Region III to IV: CSH consumed; calcite buffered.
GW + CSH at pH 11.04 (oxidized concrete, unaged; Region III per Ochs et al., 2016)	11.8 to 11.0	6	6	6	Region I to III: CSH + Increasingly calcite buffered. Region II (portlandite) negligible because Ca/Si < 1.0.
	11.0	Saturation of incoming GW with CSH limits dissolution of CSH in saltstone.			Transition to Region IV does not occur.
SDU 2/6/7 Concrete Case	**Value Range (pH)**	**Defensible Estimate 178 µeq/g (Pore Volumes)**	**Compliance Estimate 209 µeq/g (Pore Volumes)**	**Best Estimate 239 µeq/g (Pore Volumes)**	**Geochemical Controls on Transition**
GW at pH 5.4	11.1 to 10.5	5875	5855	5840	Region III (cont'd): CSH consumed to Ca-carboaluminate buffered.
	11.1 to 9.1	7610	7590	7570	Region III to IV: Ca-carboaluminate consumed to calcite buffered.

[1] Regions I through IV represent the four states of cement degradation as defined by Ochs et al, (2016). Region I (13.5 > pH > 12.5) pore fluid composition dominated by Na^+, K^+, and OH^- leaching; if present, portlandite solubility is low when pH > 12.5. Region II (pH 12.5) pore fluid composition controlled by dissolution of portlandite; this region appears to be absent or minimally present (one to two pore volumes) for saltstone and SDU concrete because Ca/Si < 1.0. Region III (12.5 > pH > 10) pore fluid composition controlled by incongruent dissolution of CSH phases to form calcite via the net overall reaction: $CaSiO_3 \cdot H_2O_{(s)} + H_2CO_{3(aq)} = CaCO_{3(s)} + SiO_{2(aq)} + 2H_2O$. Region IV (pH < 10) pore fluid composition controlled by calcite.

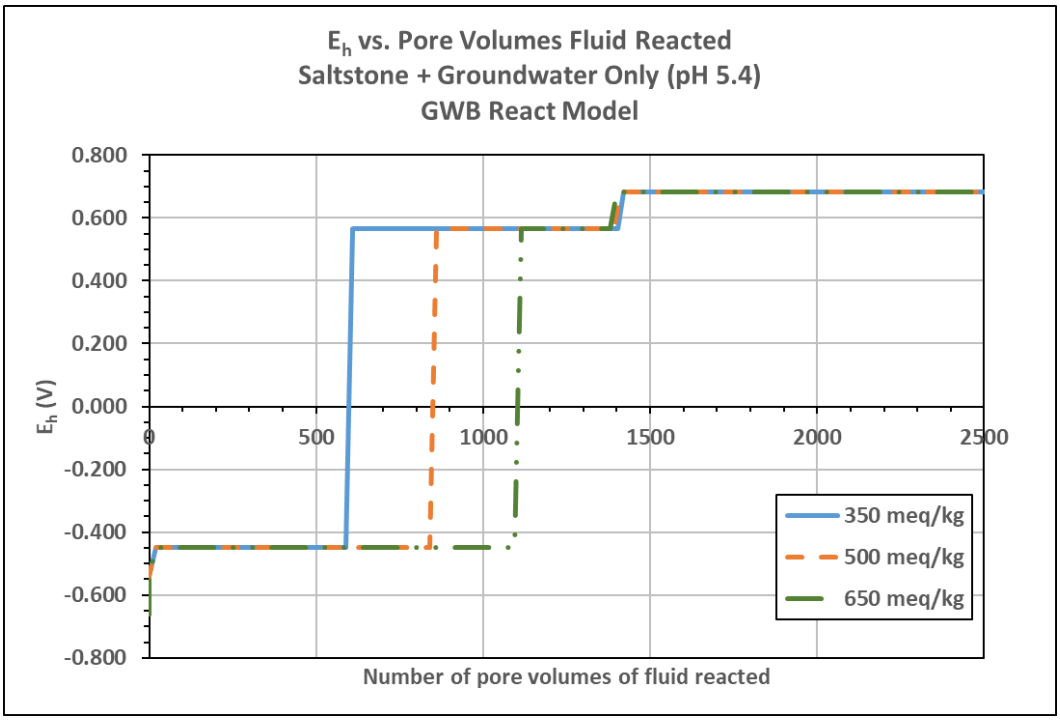

Figure 3-1. Redox Potential vs. Number of Pore Volumes of pH 5.4 Groundwater Reacted with Saltstone.

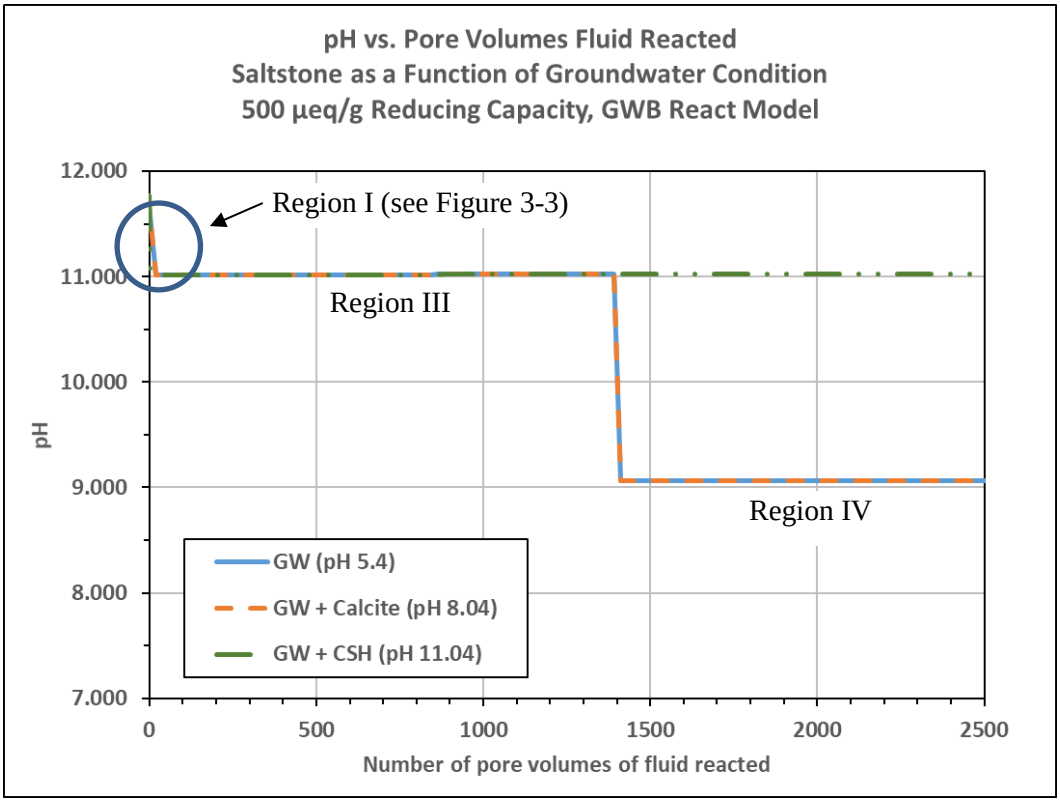

Figure 3-2. pH vs. Number of Pore Volumes of Different Groundwaters Reacted with Saltstone.

Figure 3-3 highlights the first pH transition for saltstone reacting with pH 5.4 GW for the Defensible, Compliance, and Best-Estimate Reducing-Capacity scenarios. The first transition occurs at approximately six pore volumes as noted in Table 3-2. As expected, the pH profiles are insensitive to the assumed reducing capacity of the saltstone (see Figure 3-3 and Appendix B).

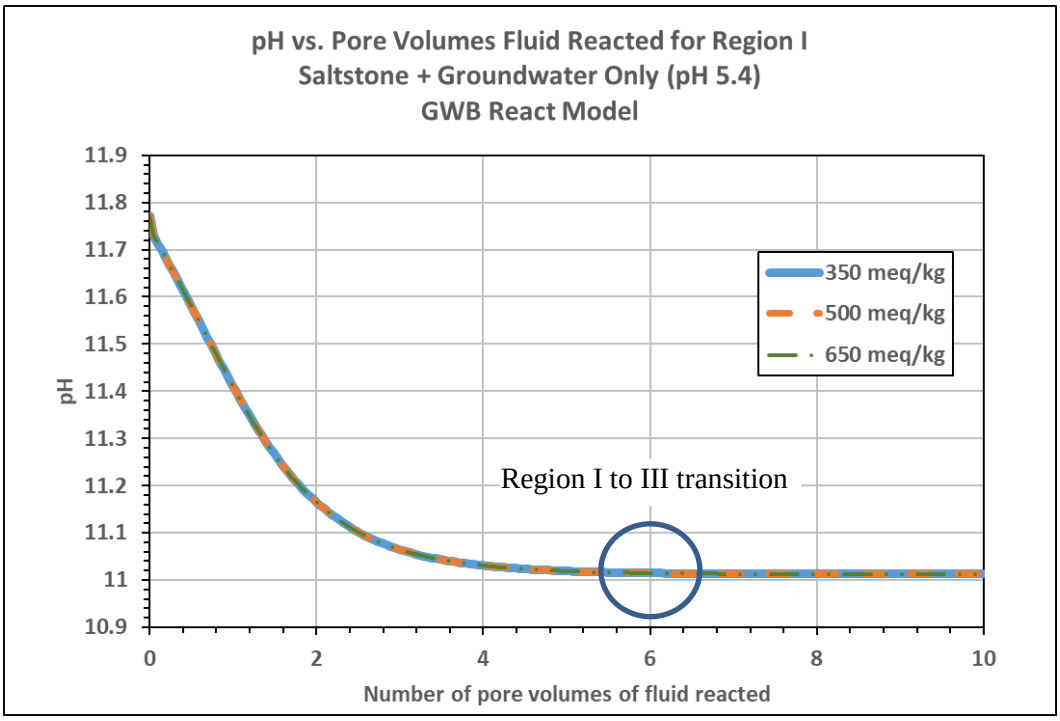

Figure 3-3. pH vs. First Ten Pore Volumes of pH 5.4 Groundwater Reacted with Saltstone.

3.2 SDU 2/6/7 Concrete Observations

The predominant E_h and pH transitions for SDU 2/6/7 concrete occur approximately four to six times later than for saltstone (i.e., approximately four to six times the number of pore volumes) primarily because of SDU concrete's 6X lower porosity (0.11 m^3 pores/m^3 total vs. 0.656 m^3 pores/m^3 total for saltstone). The delay in both transitions, however, is partially offset by SDU concrete's 5% to 45% lower mass of pyrrhotite and CSH compared to saltstone (see Table 2-7). Like saltstone, the pH transitions for SDU concrete are relatively insensitive to the assumed reducing capacity.

Figure 3-4 displays the E_h profiles for SDU 2/6/7 concrete reacted with GW at pH 5.4 for the Defensible, Compliance, and Best-Estimate Reducing-Capacity scenarios. Figure 3-5 presents the pH profiles for SDU 2/6/7 concrete reacted with GW at pH 5.4 for the Defensible, Compliance, and Best-Estimate Reducing-Capacity scenarios. As noted above, the first pH transition for SDU concrete does not represent a switch in the cement degradation region but rather a change in geochemical control from CSH buffered to Ca-carboaluminate buffered. The second pH transition, on the other hand, is important because it represents a loss in the acid neutralization capacity of the concrete and a transition from cement degradation Region III to IV as defined by Ochs et al. (2016).

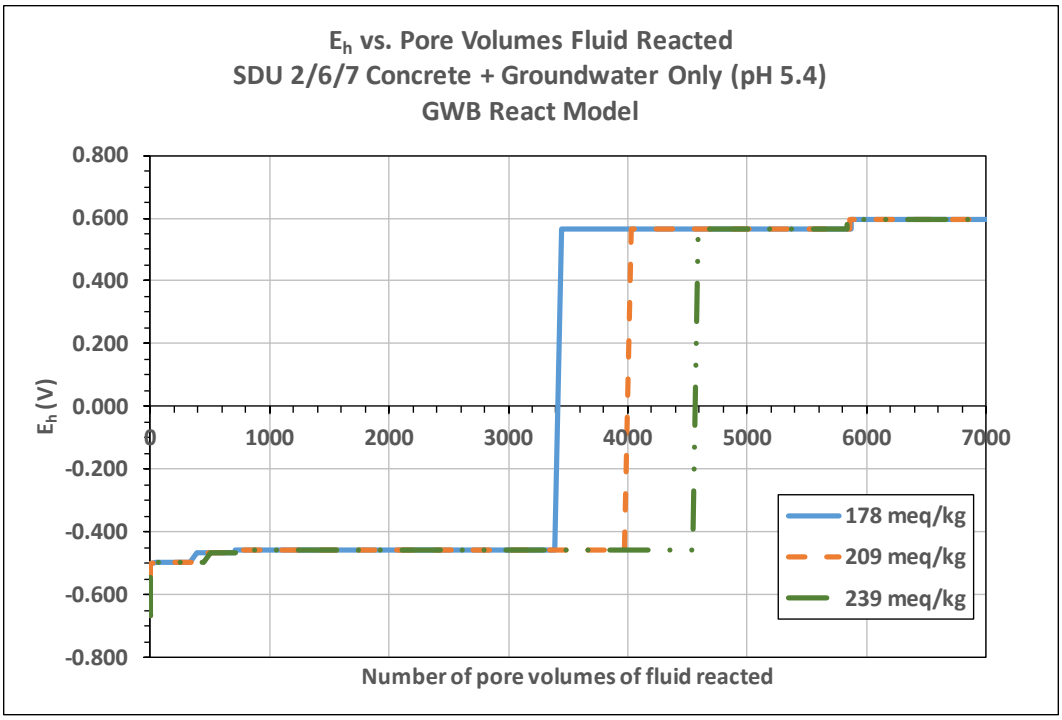

Figure 3-4. Redox Potential vs. Number of Pore Volumes of pH 5.4 Groundwater Reacted with SDU 2/6/7 Concrete.

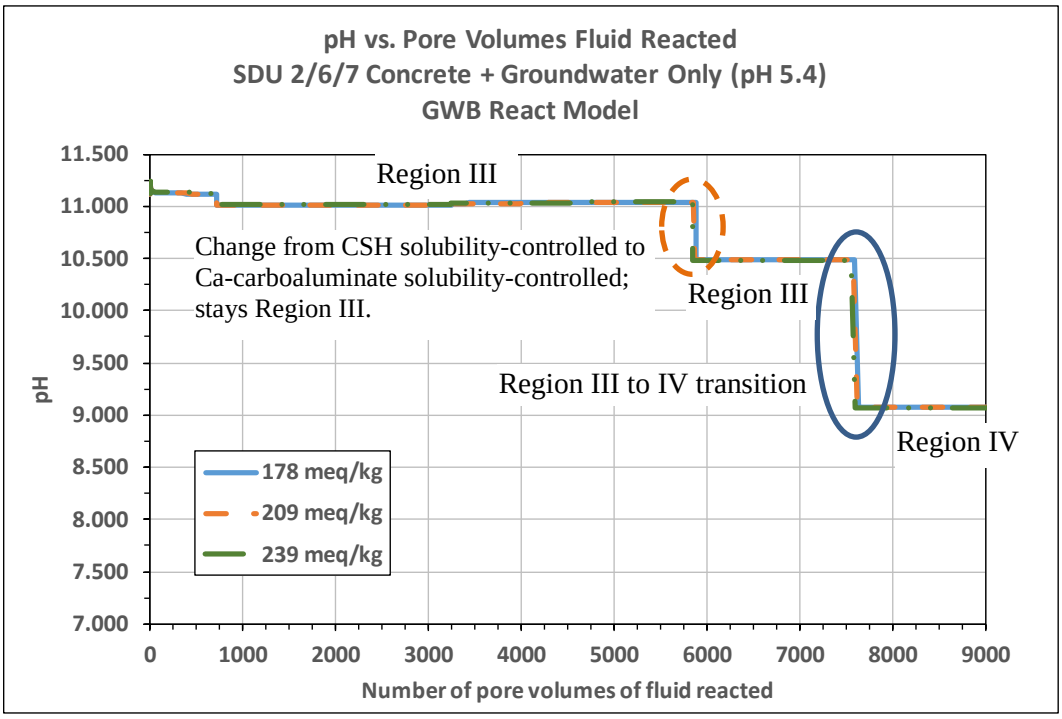

Figure 3-5. pH vs. Number of Pore Volumes of pH 5.4 Groundwater Reacted with SDU 2/6/7 Concrete.

3.3 Model Limitations

There is moderate uncertainty in the number of pore volumes calculated for the E_h and pH transitions. Uncertainties include:

- An assumption of chemical equilibrium in the GWB model leads to distinct step changes in E_h and pH (i.e., all dissolution and precipitation reactions go to completion immediately and all redox couples in the system are at equilibrium). Not all competing redox couples in natural systems reach chemical equilibrium due to kinetic constraints; therefore, small changes in E_h and changes occurring at early pore volumes should be viewed with caution. Rate-limited dissolution of minerals in the saltstone and SDU concrete will impact the pH transitions, which would result in more gradual transitions over time rather than step changes.
- Because CSH dissolves incongruently, its molecular formula will evolve as it reacts with acidity in the groundwater. This will lead to a gradual change in the mass of acid that CSH can neutralize as it ages (Denham, 2008).
- Heterogeneous distribution of BFS in the waste form and concrete could also result in deviation from a step change in E_h (Denham, 2008).
- The GWB **React** model assumes that 100% of the minerals in the saltstone and SDU concrete are fully hydrated and available for reaction with infiltrating GW. If this is not true due to fracturing or occlusion of portions of the cementitious materials from infiltrating fluid, the number of pore volumes it takes to reach the E_h and pH transition points decreases. Also, if a portion of the cementitious material remains isolated from infiltrating fluid, the associated inventory of radionuclides also remains isolated and will only be mobile by diffusional processes (Denham, 2008).
- Degradation of cementitious materials via other chemical processes is also expected to occur on a timescale of several hundred to several thousand years under SRS exposure conditions (Flach, 2018). The three most likely degradation processes, which are not addressed in this analysis, include sulfate attack, carbonation-influenced steel corrosion, and decalcification (primary constituent leaching). The impact of these chemical degradation routes on the E_h and pH transitions is unknown.

Taken together, the above processes will transform the step changes predicted by the equilibrium model to more gradual E_h and pH transitions that extend over a longer period.

4.0 Conclusions

An equilibrium reaction path model was developed and executed within The Geochemist's Workbench® software to estimate the number of pore volumes of groundwater required to chemically degrade the reducing cementitious materials that compose saltstone and SDU 2/6/7 concrete. The two assumed degradation mechanisms are oxidation of solid-phase pyrrhotite (FeS) by dissolved oxygen in groundwater as indicated by changes in redox potential and acidification of solid-phase CSH by carbonic acid as indicated by changes in pH.

Table 4-1 presents a condensed summary of the E_h and pH pore volume transitions predicted for saltstone and SDU 2/6/7 concrete. Little difference was seen in the E_h and pH transition profiles for the three GW scenarios. In addition, pH transition profiles for both saltstone and SDU 2/6/7 concrete are insensitive to the assumed solid-phase reducing capacity. The E_h and Region III-to-IV pH transitions for saltstone occur approximately four to six times earlier than they do for SDU 2/6/7 concrete, mainly because of saltstone's six times greater porosity which is partially offset by saltstone's 5% to 45% greater mass of pyrrhotite and CSH compared to SDU concrete (see Table 2-7).

Key uncertainties in the GWB model include assumptions associated with chemical equilibrium vs. rate-limited transformations, congruent vs. incongruent dissolution of CSH, homogeneous vs. heterogeneous distribution of blast furnace slag in saltstone, complete vs. partial hydration of cementitious minerals, and degradation of cementitious materials via other chemical processes including sulfate attack, carbonation-influenced steel corrosion, and decalcification. These uncertainties will have a moderate impact on the predicted E_h and pH transitions.

Table 4-1. Predicted E_h and pH Transitions for Saltstone and SDU 2/6/7 Concrete.

Case	E_h Transition				pH Transition	
	Value Range (mV)	Defensible Estimate (Pore Vol.)	Compliance Estimate (Pore Vol.)	Best Estimate (Pore Vol.)	Value Range (mV)	Pore Volume
Saltstone (all GW scenarios)	-660 to +566	600	850	1100	11.8 to 11.0 (Region I to III)	6
					11.8 to 9.1 (Region III to IV)	1400
SDU 2/6/7 Concrete (GW pH 5.4)	-660 to +565	3400	4000	4600	11.1 to 10.5 (Region III)	5850
					11.1 to 9.1 (Region III to IV)	7600

5.0 References

Aqueous Solutions LLC (2016) The Geochemist's Workbench®, Release 10.0.10. Champaign, IL.

Bennett, D. G., Read, D., Atkins, M., and Glasser, F. P. (1992) A Thermodynamic Model for Blended Cements. II: Cement Hydrate Phases; Thermodynamic Values and Modelling Studies. *J. Nucl. Mater.* **190**, 315-325.

Benson, C. H., and Benavides, J. M. (2018) Predicting Long-Term Percolation from the SDF Closure Cap. GENV-18-05. University of Virginia, Charlottesville, VA.

Berner, U. R. (1992) Evolution of Pore Water Chemistry During Degradation of Cement in a Radioactive Waste Repository Environment. *Waste Manag.* **12**(2-3), 201-219.

Bradbury, M. H., and Sarott, F. (1995) Sorption Database for the Cementitious Near-Field of a L/ILW Repository for Performance Assessment. PIT-MISC-0075, ISSN 1019-0643. Paul Scherrer Institute, Switzerland.

C-SPP-Z-00015 (2017) Procurement Specification C-SPP-Z-00015 dated 12/14/2017. Saltstone Disposal Site – SDU 7, Attachment 03300-A, Type V Concrete Mix Design, Identifier E 6000-8-S-3-AB (Foundation Mat Slab). Savannah River Remediation, Aiken, SC.

Denham, M. E. (2008) Estimation of E_h and pH Transitions in Pore Fluids During Aging of Saltstone and Disposal Unit Concrete. SRNL-TR-2008-00283. Savannah River National Laboratory, Aiken, SC.

Dyer, J. A. (2018) Software Quality Assurance Plan for The Geochemist's Workbench®, Release 10.0.10. Q-SQP-A-00007, Rev. 1. Savannah River National Laboratory, Aiken, SC.

Flach, G. P. (2018) Degradation of Saltstone Disposal Unit Cementitious Materials. SRNL-STI-2018-00077, Rev. 1. Savannah River National Laboratory, Aiken, SC.

Harbour, J. R., Hansen, E. K., Edwards, T. B., Williams, V. J., Eibling, R. E., Best, D. R., and Missimer, D. M. (2006) Characterization of Slag, Fly Ash, and Portland Cement for Saltstone. WSRC-TR-2006-00067, Rev. 0. Washington Savannah River Co., Aiken, SC.

Hommel, S. P. (2018) Recommended Values for Cementitious Degradation Modeling to Support Future SDF Modeling. SRR-CWDA-2018-00004, Rev. 1. Savannah River Remediation, Aiken, SC.

Hommel, S. P., and Dixon, K. D. (2018) Recommended Reducing Capacity for Saltstone for the SDF PA. SRR-CWDA-2018-00048. Savannah River Remediation, Aiken, SC.

Langton, C. A., and Missimer, D. M. (2014) X-ray Diffraction of Slag-based Sodium Salt Waste Forms. SRNL-STI-2014-00397, Rev. 1. Savannah River National Laboratory, Aiken, SC.

Millings, M. R. (2012) Summary Carbon Dioxide in Water Table Wells and the Vadose Zone at SRS. SRNL-L3200-2012-00017. Savannah River National Laboratory, Aiken, SC.

Millings, M. R., and Denham, M. E. (2012) Background Water Table Chemistry in the General Separations Area. SRNL-L3200-2012-00022. Savannah River National Laboratory, Aiken, SC.

Millings, M. R., Denham, M. E., and Drown, W. A. (2012) Software Quality Assurance Plan for The Geochemist's Workbench®. Q-SQP-A-00007, Rev. 0. Savannah River National Laboratory, Aiken, SC.

Ochs, M., Mallants, D., and Wang, L. (2016) Radionuclide and Metal Sorption on Cement and Concrete. Springer International Publishing, Switzerland.

Park, J-Y., and Batchelor, B. (2002) General Chemical Equilibrium Model for Stabilized/Solidified Wastes. *J. Environ. Eng.* **128**(7)**,** 653-661.

Reardon, E. J., (1990) An Ion Interaction Model for the Determination of Chemical Equilibria in Cement/Water Systems., *Cement Concrete Res.* **20**(2), 175-192.

Roberts, K. A., and Kaplan, D. I. (2009) Reduction Capacity of Saltstone and Saltstone Components. SRNL-STI-2009-00637, Rev. 0. Savannah River National Laboratory, Aiken, SC.

SIMCO Technologies Inc. (2010) Washington Savannah River Company Subcontract no. AC48992N Report. Task 6 – Characterization of a Wasteform Mixture. SIMCO Technologies Inc., Quebec, Canada.

SIMCO Technologies Inc. (2012) Washington Savannah River Company Subcontract no. AC81850N Report. Vault Concrete Characterization. SIMCO Technologies Inc., Quebec, Canada.

This Page Intentionally Blank

Appendix A. Chemical Compositions of Dry Mix Ingredients

This Page Intentionally Blank

Table A-1. Chemical Compositions Considered for Portland Cement.

Cement

Oxide	Simco (2010) Type I/II	Simco (2012) Type I/II	Simco (2012) Type V	Harbour (2006) Portland,1	Harbour (2006) Portland,2	Average g / 100 g	Normal-ized g / 100 g
CaO	64.3	64.8	63.8	64.9	63.0	64.16	64.79
SiO2	21.0	20.9	21.0	20.5	20.3	20.74	20.94
Al2O3	4.91	4.80	3.82	5.4	5.2	4.826	4.87
Fe2O3	3.50	3.43	4.75	3.7	3.8	3.836	3.87
SO3	2.64	1.75	1.15	3.2	3.3	2.408	2.43
MgO	0.95	1.05	2.60	1.2	1.2	1.4	1.41
K2O	0.37	0.54	0.61	0.5	0.7	0.544	0.55
Na2O	0.09	0.22	0.15	0.1	0.2	0.152	0.15
TiO2	NR	NR	NR	0.3	0.3	0.3	0.30
LOI* / volatiles	1.32	1.13	0.84	0	0	0.658	0.66
Total	99.08	98.62	98.72	99.8	98.0	99.024	100.00

* Loss On Ignition

Table A-2. Chemical Compositions Considered for Blast Furnace Slag.

Slag

Oxide	Simco (2010) Holcim	Simco (2012) Holcim	Harbour (2006) Batch 1	Harbour (2006) Batch 2	Average g / 100 g	Normal-ized g / 100 g
CaO	35.8	37.8	38.5	35	36.775	36.84
SiO2	39.1	39.6	37.9	40.4	39.25	39.32
Al2O3	10.1	7.61	8.4	6.6	8.1775	8.19
Fe2O3	0.36	0.47	0.4	0.3	0.3825	0.38
SO3	1.99	1.05	1	2.5	1.635	1.64
MgO	12.6	12.2	12.9	13.1	12.7	12.72
K2O	0.27	0.47	0.3	0.5	0.385	0.39
Na2O	0.22	0.28	0.3	0.3	0.275	0.28
TiO2	NR	NR	0.4	0.3	0.35	0.35
LOI* / volatiles	0	-0.45	0	0	-0.1125	-0.11
Total	100.44	99.03	100.1	99	99.8175	100.00

* Loss On Ignition

Table A-3. Chemical Compositions Considered for Fly Ash.

Fly Ash

Oxide	Simco (2010) Class F	Simco (2012) Class F	Harbour (2006) Batch 1	Harbour (2006) Batch 2	Average g / 100 g	Normal-ized g / 100 g
CaO	1.41	1.32	0.7	0.6	1.0075	1.02
SiO2	53.1	54.5	54.2	56.8	54.65	55.34
Al2O3	28.4	28.1	28.6	28.6	28.425	28.78
Fe2O3	7.99	8.65	6	5.6	7.06	7.15
SO3	0	0	0.1	0.3	0.1	0.10
MgO	1	1.19	0.9	0.8	0.9725	0.98
K2O	2.99	2.82	2.6	2.5	2.7275	2.76
Na2O	0.44	0.41	0.3	0.4	0.3875	0.39
TiO2	NR	NR	1.6	1.4	1.5	1.52
LOI* / volatiles	2.39	1.41	2.5	1.4	1.925	1.95
Total	97.72	98.4	97.5	98.4	98.755	100.00

* Loss On Ignition

Table A-4. Chemical Compositions Considered for Silica Fume.

Silica Fume

Oxide	Simco (2010) Grace	Simco (2012) Grace	Harbour (2006) Batch 1	Harbour (2006) Batch 2	Average g / 100 g	Normal-ized g / 100 g
CaO	NR	0.6	NR	NR	0.6	0.60
SiO2	NR	95	NR	NR	95	94.78
Al2O3	NR	0.18	NR	NR	0.18	0.18
Fe2O3	NR	0.07	NR	NR	0.07	0.07
SO3	NR	0.18	NR	NR	0.18	0.18
MgO	NR	0.22	NR	NR	0.22	0.22
K2O	NR	0.48	NR	NR	0.48	0.48
Na2O	NR	0.18	NR	NR	0.18	0.18
TiO2	NR	NR	NR	NR	0	0.00
LOI* / volatiles	NR	3.32	NR	NR	3.32	3.31
Total	0	100.23	0	0	100.23	100.00

* Loss On Ignition

Appendix B. Additional E_h and pH Profiles for Saltstone and SDU 2/6/7 Concrete Cases

This Page Intentionally Blank

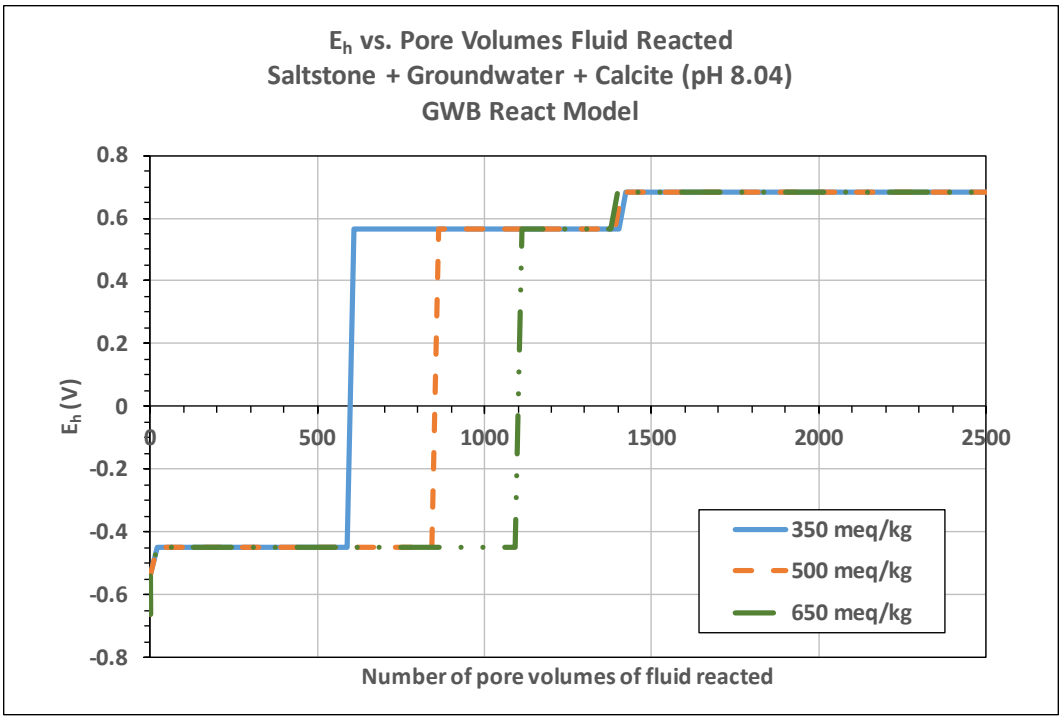

Figure B-1. Redox Potential vs. Number of Pore Volumes of "Groundwater + Calcite at pH 8.04" Reacted with Saltstone.

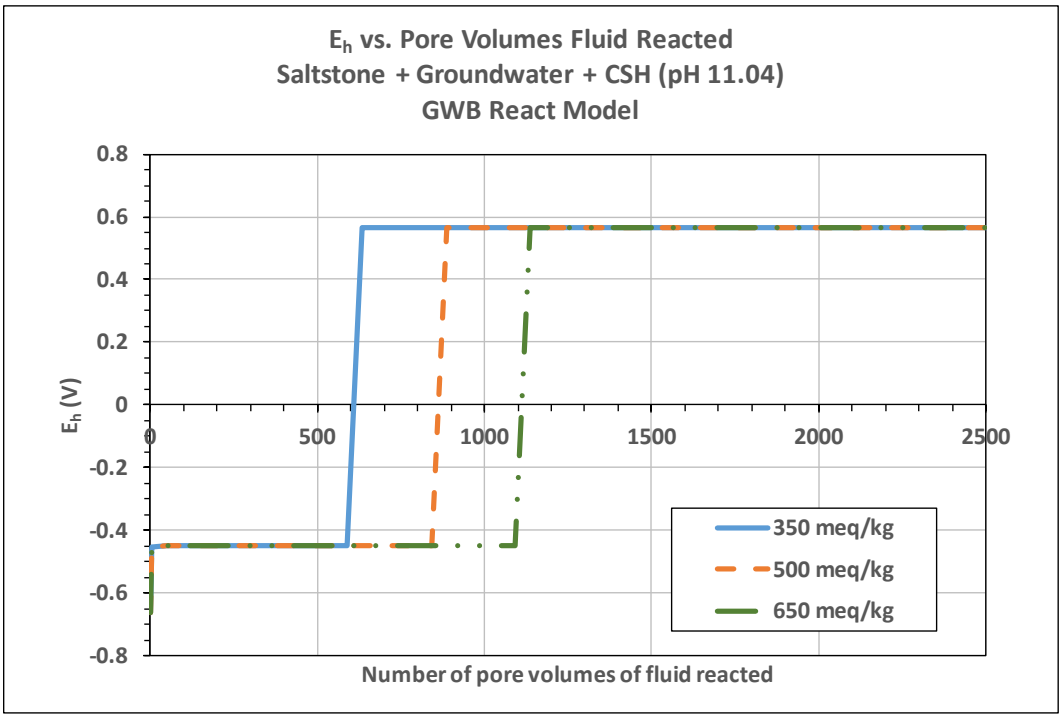

Figure B-2. Redox Potential vs. Number of Pore Volumes of "Groundwater + CSH at pH 11.04" Reacted with Saltstone.

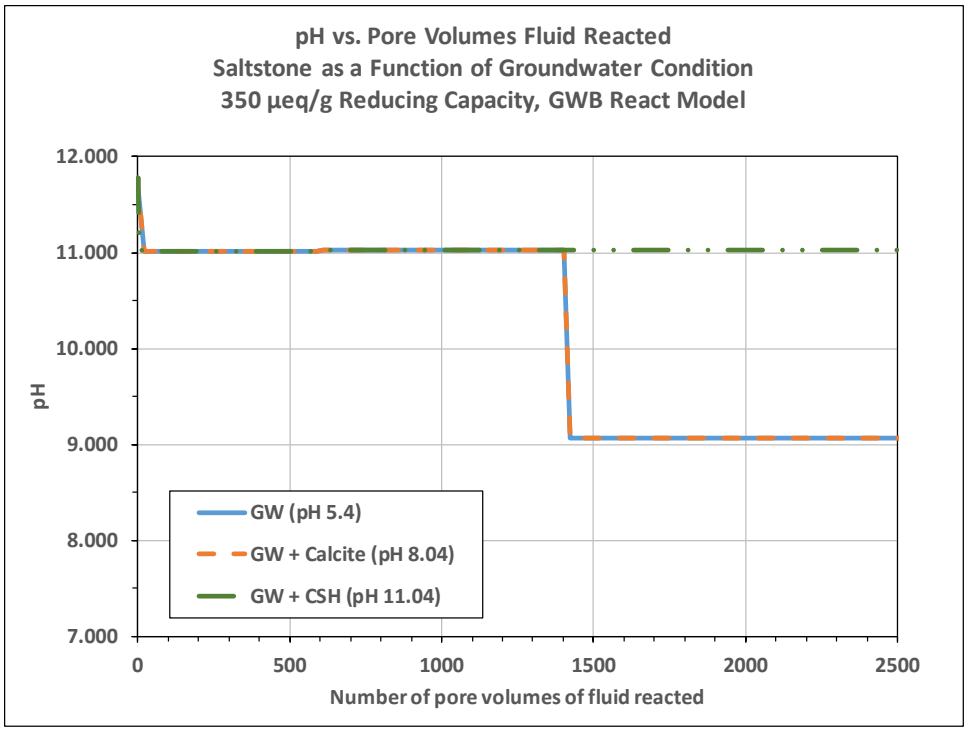

Figure B-3. pH vs. Number of Pore Volumes of Different Groundwaters Reacted with Saltstone at 350 µeq/g Reducing Capacity.

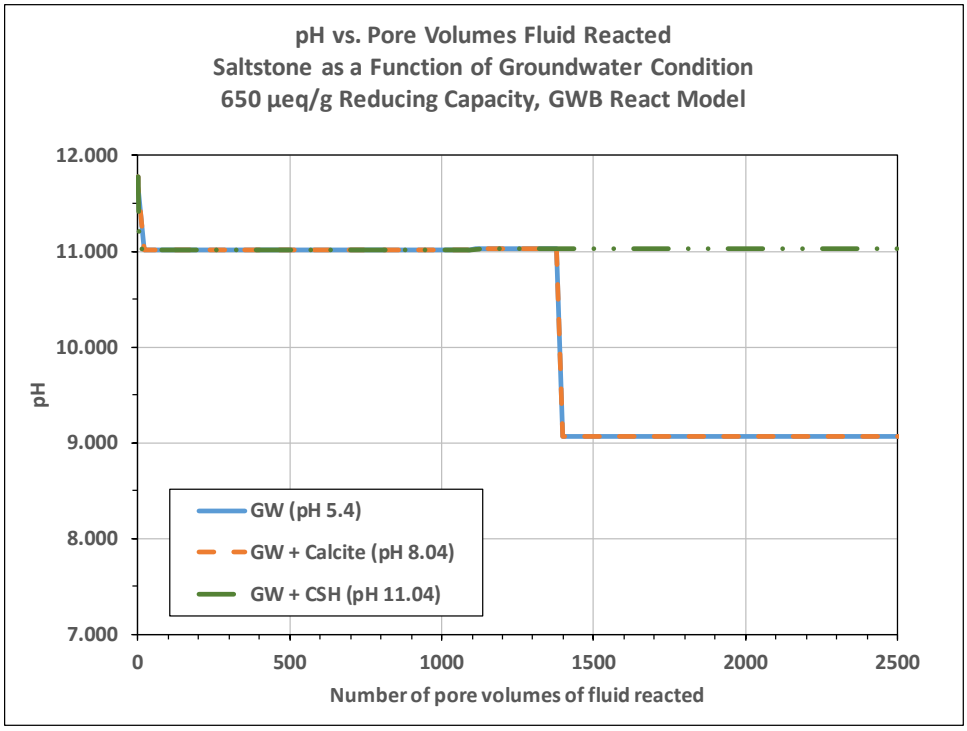

Figure B-4. pH vs. Number of Pore Volumes of Different Groundwaters Reacted with Saltstone at 650 µeq/g Reducing Capacity.

This Page Intentionally Blank

Distribution:

timothy.brown@srnl.doe.gov
tom.butcher@srnl.doe.gov
tim.coffield@srs.gov
alex.cozzi@srnl.doe.gov
david.crowley@srnl.doe.gov
thomas.danielson@srnl.doe.gov
john.dickson@srnl.doe.gov
david.dooley@srnl.doe.gov
james.dyer@srnl.doe.gov
a.fellinger@srnl.doe.gov
samuel.fink@srnl.doe.gov
gregory.flach@srnl.doe.gov
kevin.fox@srnl.doe.gov
luther.hamm@srnl.doe.gov
erich.hansen@srnl.doe.gov
thong.hang@srnl.doe.gov
connie.herman@srnl.doe.gov
steven.hommel@srs.gov
vijay.jain@srs.gov
daniel.kaplan@srnl.doe.gov
dien.li@srs.gov
barry.lester@srs.gov
jeremiah.mangold@srs.gov
john.mayer@srnl.doe.gov
daniel.mccabe@srnl.doe.gov
nancy.halverson@srnl.doe.gov
frank.pennebaker@srnl.doe.gov
luke.reid@srnl.doe.gov
larry.romanowski@srs.gov
kent.rosenberger@srs.gov
ira.stewart@srs.gov
kevin.tempel@srs.gov
steven.thomas@srs.gov
david.watkins@srs.gov
boyd.wiedenman@srnl.doe.gov
bill.wilmarth@srnl.doe.gov
jennifer.wohlwend@srnl.doe.gov
Records Administration (EDWS)
T. N. Foster, EM File, 773-42A – Rm. 243
(1 file copy and 1 electronic copy)